C. R. Geoscience 346 (2014) 233–243

Contents lists available at ScienceDirect

Comptes Rendus Geoscience

www.sciencedirect.com

Petrology, geochemistry

Zircon crystal morphology and internal structures as a tool for constraining magma sources: Examples from northern Portugal Variscan biotite-rich granite plutons

Helena C. Brites Martins [a,*], Pedro P. Simões [b], Joana Abreu [a]

[a] Geology Centre/Department of Geosciences, Environment and Spatial Planning, Faculty of Sciences, Porto University, Rua do Campo Alegre, 4169-007 Porto, Portugal
[b] Department of Earth Science, Geology Centre Porto University, Minho University, 4710-057 Braga, Portugal

ARTICLE INFO

Article history:
Received 2 June 2014
Accepted after revision 10 July 2014
Available online 25 October 2014

Keywords:
Zircon
Granite
Typology
Variscan
Portugal

ABSTRACT

In northern Portugal, large volumes of granitoids were emplaced during the last stage (D_3) of the Variscan orogeny and display a wide range of petrological signatures. We studied the morphologies and internal structures of zircons from syn-, late- and post-D_3 granitoids. The sin-D_3 granitoids include the Ucanha–Vilar, Lamego, Felgueiras, Sameiro, and Refoios do Lima plutons, the late- and post-D_3 granitoids are represented by the Vieira do Minho and the Vila Pouca de Aguiar plutons, respectively. Typological investigations after Pupin (1980) along with scanning electron microprobe imaging reveal that the external morphology of zircon changes consistently with a decrease in the crystallization temperature. Zircon populations from the Refoios do Lima and the Vieira do Minho granites show gradual changes in the internal morphologies and their typologic evolution trends are consistent with their mainly crustal origin. The Sameiro, Felgueiras, Lamego and Ucanha-Vilar granites have more complex internal and external morphology and typological evolution trends that cross the domain of the calc-alkaline to the aluminous granites compatible with a mixing process. Finally, the morphological types of the Vila Pouca de Aguiar granites are found both in calc-alkaline and sub-alkaline granites and their typological evolutionary trends follow the calc-alkaline/sub-alkaline trend, suggesting crustal sources with some mantle contribution.

1. Introduction

Zircon is an important accessory mineral of granitic rocks, very resistant to weathering and metamorphic processes. The different zircon crystal morphologies that characterize different kinds of granites depend on magma chemistry, changes in the temperature of crystallization and aluminium-alkali balance (Pupin, 1976; Pupin and Turco, 1972, 1975); therefore, zircon populations have been used as tracers of granitic magma petrogenesis. Among several morphological parameters, the crystal habit is the most variable and carry important petrogenetic information, as pointed out by Pupin and Turco (1972, 1975) and Pupin (1976, 1980, 1985, 1988). However, the principles of Pupin's method were challenged by several authors (e.g., Benisek and Finger, 1993; Vavra, 1990, 1993) stating that zircon crystal morphologies could only reflect the latest stages of granitoid evolution. According to Vavra (1990, 1993), the external morphology of a single crystal can change a number of times during a single growth event

* Corresponding author. Geology Centre/Department of Geosciences, Environment and Spatial Planning, Faculty of Sciences, Porto University, Rua do Campo Alegre 4169-007 Porto, Portugal.
E-mail address: hbrites@fc.up.pt (H.C. Brites Martins).

http://dx.doi.org/10.1016/j.crte.2014.07.004
1631-0713/

as a result of kinetic factors, such as diffusion rates and adsorption, which affect the growth rates of the crystal faces and therefore control the morphology of a growing crystal. The influence on the growth rate of different forms can be attributed to either the degree of zircon saturation or the incorporation of trace elements (Vavra, 1994). On the other hand, Benisek and Finger (1993) have shown that a relative development of the zircon prisms faces is strongly related with zircon-supersaturation of the melt, instead of the crystallization temperature.

With the present morphological zircon study, we aimed to characterize the source reservoirs involved in the generation of sin-, late- and post-D_3 biotite-rich granitoids from northern Portugal, a suite of geochemically well-characterized plutons, which have been the subject of intensive whole-rock and mineral-scale studies (Almeida et al., 2002; Dias et al., 1998, 2002; Martins et al., 2007, 2009, 2013; Simões, 2000) testing the classic "Pupin method" against the petrogenetic indications given by geochemical and isotopic data.

2. Geological setting

The central and western Iberian Peninsula constitutes a segment of the West European Variscan Fold Belt, the Iberian Massif. Tectonic characteristics of the European Variscides are those of a classical subduction–collision–obduction model – in this case, the collision of the Laurentia and the Gondwana continents, with minor intermediate blocks. The geological evolution of this segment has been described in detail by several authors (Bard et al., 1980; Dias and Ribeiro, 1995; Lagarde et al., 1992; Matte, 1991; Ribeiro et al., 1983, 1990). Three main ductile deformation phases, D1, D2 and D3, are identified in the NW Iberian Massif, responsible for the structural development of this part of the Variscan belt (Dias and Ribeiro, 1995; Noronha et al., 1979). The last phase, D4, is related to an extension regime, post-collision, with brittle deformation. During the last ductile deformation phase (D3) of the Variscan orogeny, large volumes of granitoids were emplaced in northern Portugal. This was the main period of successive generation of granites (Ferreira et al., 1987), which exhibit large compositional variability (Dias et al., 1998; Martins et al., 2009, 2013). The classification of granitoids is related to this third phase of deformation (Dias et al., 1998; Ferreira et al., 1987; Martins et al., 2009, 2011, 2013) divided into:

- syn-D_3 granitoids, 313–319 Ma (peraluminous biotite granodiorites to monzogranites and highly peraluminous two-mica leucogranites);
- late-D3 biotite-dominant granitoids, 306–311 Ma (mainly as composite massifs displaying a wide compositional range from gabbroic to granitic, being metaluminous to peraluminous);
- late- to post-D3 granitoids, ca. 300 Ma (highly peraluminous, two-mica leucogranites);
- post-D3 granitoids, 290–296 Ma (slightly metaluminous to peraluminous monzogranites occurring as zoned plutons).

Syn- and late-D3 biotite-rich granodiorites and monzogranites are the most abundant granitic rocks in northern Portugal, spatially associated with mafic microgranular enclaves and minor bodies of basic to intermediate rocks.

3. Geology and petrological signatures

The granitic plutons selected for this study are located in the central Iberian Zone, northern Portugal. They are syn-D_3 biotite granitoids, late-D_3 biotite-dominant granitoids and post-D_3 biotite granitoids (Fig. 1) whose emplacement was controlled by important tectonic regional structures like ductile shear zones or Late Variscan fragile fracturing and faulting.

3.1. Syn-D_3 biotite granitoids

This group is spatially related to the Vigo–Régua shear zone, and includes, from south to north, the Ucanha–Vilar, Lamego, Felgueiras, Sameiro and Refoios do Lima plutons.

They are porphyritic (orthoclase phenocrysts) medium-grained biotite granodiorites/monzogranites and contain quartz + plagioclase (andesine/oligoclase) + perthitic orthoclase + biotite + zircon + monazite + apatite + ilmenite ± muscovite ± allanite (+ cordierite + sillimanite in the Refoio do Lima pluton) (Dias et al., 2002; Simões, 2000). The Ucanha–Vilar is spatially associated with hm-sized granodioritic stocks. Mafic microgranular enclaves are common, although they are rare, in the Refoios do Lima pluton. The U–Pb zircon geochronological data for Ucanha–Vilar, Lamego, Sameiro and Refoios do Lima granites have given crystallization ages between 313 and 321 Ma, with almost concordant monazite ages of 317 and 318 Ma.

They are interpreted as moderately peraluminous with magnesian and alkali-calcic affinity (Frost et al., 2001), being the Refoios do Lima the most aluminous. SiO_2 contents range from 62 to 70% and are characterized by rather high Ba (720–2181 ppm), high LREE contents (La = 77–167 ppm), highly fractionated patterns (La_N/Yb_N = 32–78) and moderate negative Eu anomalies (Eu/Eu^* = 0.52–0.72). On the other hand, these granitoids display $^{87}Sr/^{86}Sr$ initial ratios and ε_{Nd} values varying in the ranges 0.7072–0.7116 and –4.4 to–6.3, respectively (Dias et al., 2002; Simões, 2000).

3.2. Late-D3 biotite-dominant granitoids

Late-D_3 biotite-dominant granitoids are represented by the Vieira do Minho pluton. This pluton is composite and consists of two different granite units (Almeida et al., 2002; Martins et al., 2013): the Vieira do Minho granite (VM) is a coarse-grained monzogranite and the Moreira de Rei (MR) granite a medium-grained monzogranite.

The two granites are porphyritic and present the following mineral association: quartz + perthitic K-feldspar (orthoclase or microcline) + plagioclase (oligoclase-andesine) + biotite ± muscovite. Andalusite and cordierite were also observed, but only in one sample from the Vieira do Minho granite. Apatite, zircon, titanite, ilmenite, monazite

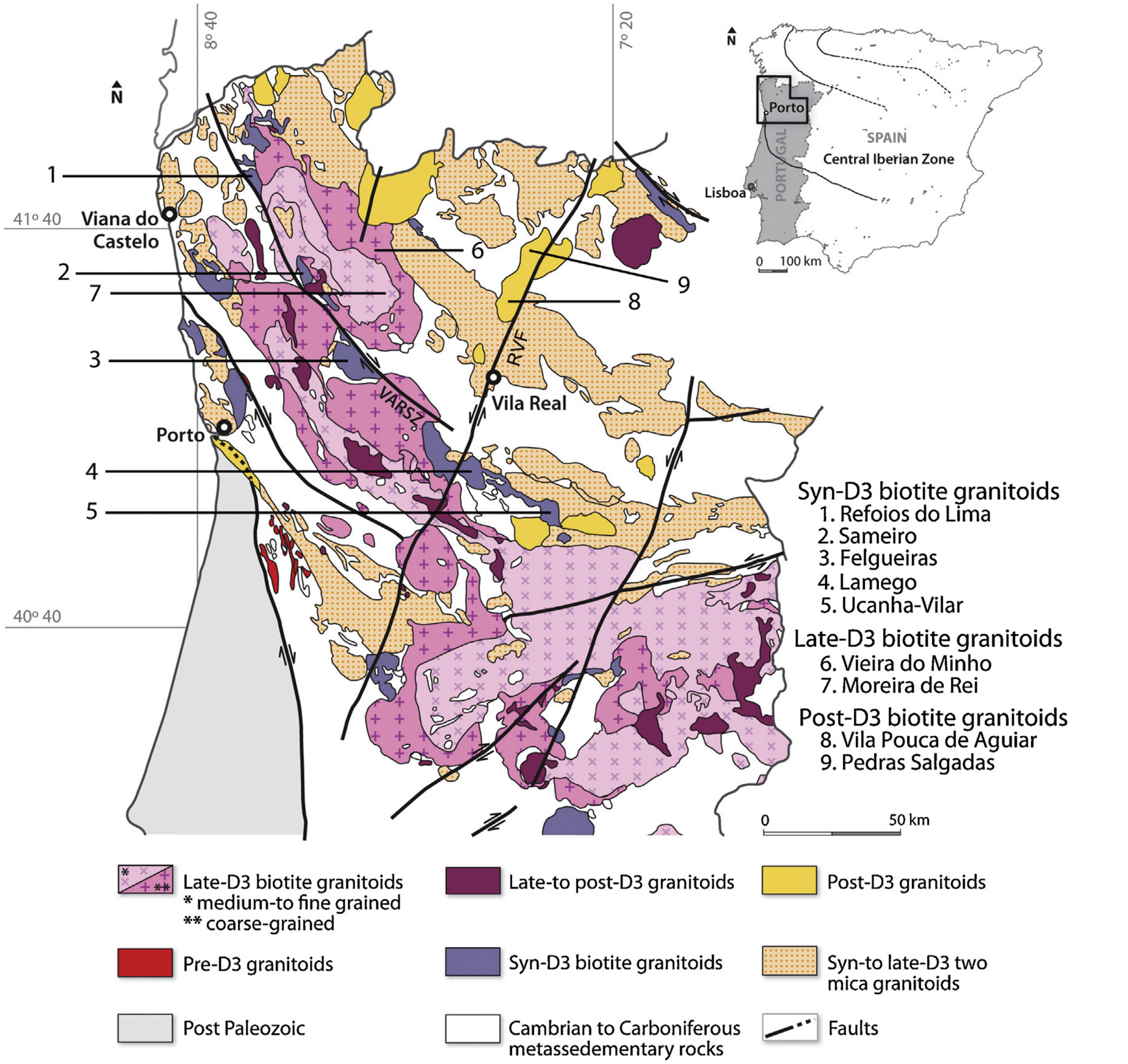

Fig. 1. (Color online.) Geological distribution of Variscan syn- to post-orogenic granitoids in the central Iberian Zone, northern Portugal (Ferreira et al., 1987 modified) with location of the studied plutons. D_3-last ductile deformation phase; VARSZ, Vigo–Amarante–Régua Shear Zone; RVF, Régua–Verin Fault.

(only in VM) and thorite + allanite (in MR) can be found as accessory phases. The gradational contacts between the Vieira do Minho and Moreira de Rei granite indicate an almost synchronous emplacement. The U–Pb isotopic analyses carried out on zircon and monazite fractions from the Vieira do Minho granite indicate a crystallization age of 310 ± 2 Ma (Martins et al., 2013). The Moreira de Rei granite has been dated by Dias et al. (2002) yielding an age of 308 ± 4 Ma. Geochemically (Frost et al., 2001), this group is represented by peraluminous granites with alkali-calcic signature. However, the VM granite plots mostly in the ferroan field and the MR in the magnesian field. The VM and the MR granites are characterized by a high and restricted SiO_2 range from 67 to 73 wt. %, and they present a moderate REE fractionated patterns (La_N/Yb_N = 13–22) and moderate negative Eu anomalies (Eu/Eu^* = 0.42–0.61). On the other hand, both granitoids have similar ε_{Nd} values (VMG = −5.2 to −5.7; MRG = −4.98 to −5.96), but the VM granite is slightly more enriched in $(^{87}Sr/^{86}Sr)_i$ = 0.7087–0.7098 as well as in $\delta^{18}O$ in the range from 10.6‰ to 11.0‰ than the MR granite with $(^{87}Sr/^{86}Sr)_i$ = 0.7064–0.7075 and $\delta^{18}O$ = 9.9‰–10.5‰ (Martins et al., 2013).

3.3. *Post-D3 biotite granitoids*

The post-D_3 Vila Pouca de Aguiar pluton has a NNE–SSW (N20 to N30) elongated shape, with the same orientation of the Late Variscan D_4 brittle structure, the Régua–Verin fault. It is also a composite massif with two main different biotite-rich granite units: the Vila Pouca de Aguiar granite (VPA), medium-coarse-grained with some mafic microgranular enclaves, and the Pedras Salgadas granite (PS), medium to fine grained. Both granites are porphyritic and contain quartz + perthitic K-feldspar (orthoclase or microcline) + plagioclase (oligoclase–andesine) + biotite + ilmenite + apatite + zircon + allanite ± monazite ± xenotime. The field relationships indicate a synchronous magmatic emplacement of these granites. The U–Pb isotopic analyses of zircon fractions from the Vila Pouca de Aguiar granite give an emplacement age of 299 ± 3 Ma (Martins et al., 2007, 2009). These granites are characterized by a weakly peraluminous character and by calc-alkaline to alkali-calcic signatures (Frost et al., 2001). The SiO_2 content ranges from 71 to 74% and they have wing-shaped patterns with $(La/Yb)_N$ ranging from 3 to 9, with moderate negative Eu anomaly ($Eu/Eu^* = 0.29–0.50$). These granites display weakly evolved isotopic compositions ($(^{87}Sr/^{86}Sr)_i = 0.7044–0.7077$ and $\varepsilon_{Nd} = -2.0$ to -2.6), and a whole-rock oxygen isotope ($\delta^{18}O$ VSMOW) ranging from +9.7‰ to +11.0‰ (Martins et al., 2009).

4. Analytical methods

Zircon populations are separated from granites using the following procedure: crushing of the sample, sieving to obtain zircon grains with sizes corresponding to the fraction between 0.050 and 0.200 mm, and use of heavy liquids (bromoform and methylene iodide) followed by using an electromagnetic separator (Frantz). The zircon crystals are then mounted on glass slides with Canada balsam and studied under the transmitted light microscope at 250 × magnification. For each of the granitic rock samples studied, the typologic distribution has been determined on the basis of the examination of at least 100 unbroken zircon crystals. Representative zircon grains were handpicked and embedded in epoxy resin and polished in order to be observed by back-scattered electron (BSE) imaging by electron microscopy. This has been carried out at Porto University (Fei Quanta 400 FEG ESEM) and at Minho University (Leica Cambridge Stereoscan 360).

5. Typology

The crystal system of zircon is tetragonal, and its crystal symmetry is tetragonal or ditetragonal, dipyramidal. The combination of the most common crystalline faces (pyramids {101}, {211} and prisms {100}, {110}) is the basis of zircon typology (Pupin and Turco, 1972). The extra {301} pyramid can exist, but with a minor development. Main types and subtypes are reported in a square board with two variables (IA–IT diagram), depending on the relative development of prismatic and pyramidal crystal faces (Fig. 2).

The *A* index (IA) is correlated with the Al/(Na + K) ratio and with the development of pyramidal faces. The {211}, {101} and {301} pyramids are respectively well-developed in aluminous, alkaline and peralkaline medium, respectively. The *T* index (IT) is correlated with the temperature of zircon crystallization, which is responsible for the development of the prismatic faces. A high *T* index ({100} prim) indicates a higher temperature than a low T index ({110} prism) does. A given zircon population will be characterized by:

- a typological distribution (frequency of each type and subtype);
- a TET (Typological Evolutionary Trend);
- a mean point (A, T) calculated as: $IA = \sum IA \times n_{IA}$, $IT = \sum IT \times n_{IT}$, where n_{IA} and n_{IT} are the respective frequencies for each value of IA or IT envisaged between 100 and 800, with $\sum n_{IA} = \sum n_{IT} = 1$.

The TET represents the chronology and evolution of the different types and subtypes during the magmatic stage and is defined as the mean points of IA calculated for each value of IT (Pupin, 1988). For the typological study of zircon populations (Pupin, 1980), at least 100 euhedral crystals were chosen randomly and identified for each sample.

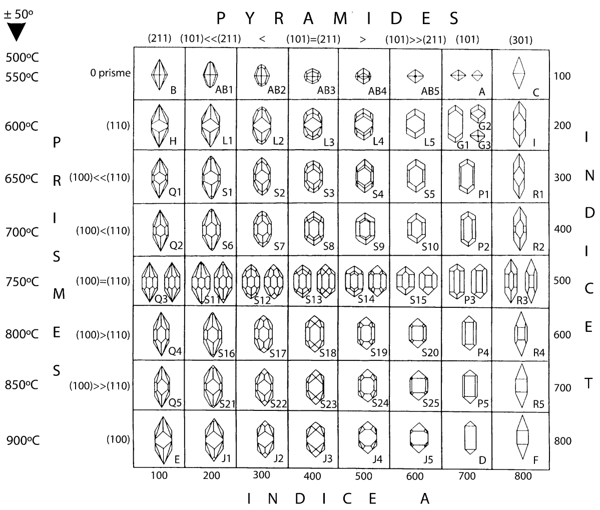

Fig. 2. Zircon typological classification proposed by Pupin (1980). Index A reflects the Al/alkali ratio, controlling the development of zircon pyramids, whereas temperature affects the development of different zircon prisms.

Pupin (1980) proposed that the typologic study of zircon populations from granitic rocks can be used as a genetic classification, with three main divisions as:

- granitoids of crustal (or mainly crustal) origin;
- hybrid (crustal and mantle origin) granitoids;
- granitoids of mantle (or mainly mantle) origin.

On the typology diagram, granitoids of different origin show different populations and distinct TETs.

Crustal granitoids generally include leucogranites and aluminous monzogranites with no or little basic microgranular enclaves, and are characterised by low *A* and *T* indices. The granitoids in the hybrid-group are mainly calc-alkaline or sub-alkaline monzogranites and granodiorites, typically including basic microgranular enclaves; they show zircon populations having large ranges of *A* (higher than those of crustal ones) and *T* (from very high to low) indices. Alkaline granitoids are assumed to be represented in the group of mantle or mainly mantle origin with zircon showing very high *A* and *T* index values (Pupin, 1980).

5.1. Results

5.1.1. Syn-D_3 biotite granitoids

The typological study using the methodology of Pupin (1980) shows that for Refoios do Lima (REF) granite, the main subtypes of zircons are S1, S2, S6, S7, S11, and S12 (Fig. 2), with a predominance of {211} pyramids on {101}, indicating an aluminous magmatic environment (Pupin, 1980), giving a low IA index in the range from 274 to 286 (Fig. 3a). This aluminous environment is also evidenced by the presence of cordierite and sillimanite in the granite. Most of the zircons present equally well-developed {100} and {110} prisms, with a slight predominance of the latter, giving a mean IT index in the range from 371 to 440 (Fig. 3a). According to their distribution, the population of zircons plot in the intrusive aluminous monzogranites–granodiorites domain, although one of the samples is situated in an area overlapping multiple typological domains (Fig. 3a).

In the Felgueiras (FEL) granite, most zircons are of subtypes S2, S7 and S8, while in Ucanha–Vilar (U–V) granite, S3, S7, S8 and S12 are the main subtypes of zircons (Fig. 2). They also have zircons with morphological characteristics similar to those of zircons occurring in intrusive aluminous monzogranites–granodiorites (Fig. 3), although closer to the calc-alkaline field. In fact, most of their zircons present less developed {211} pyramids than Refoios do Lima zircons, giving a higher IA index (Fig. 3a), suggesting an environment more depleted in aluminium and richer in alkalis.

For the other two syn-D3 granites, the zircon populations in Sameiro (SAM) granite are characterised mainly by S8, S12, S13, and S18 types, while in the Lamego (LAM) granite, the main types of zircons are S3, S4, S7, S8, and S18 (Fig. 2). These populations of zircons present an equal development of {101} and {211} pyramids and more variations on prisms, giving on average the highest IA index and the lower IT index. Given the morphological characteristics of their zircons, these granites reveal zircons identical to those that are found in calc-alkaline granites, although the more evolved population of Lamego zircons plots in the intrusive aluminous granodiorites–granodiorites domain (Fig. 3).

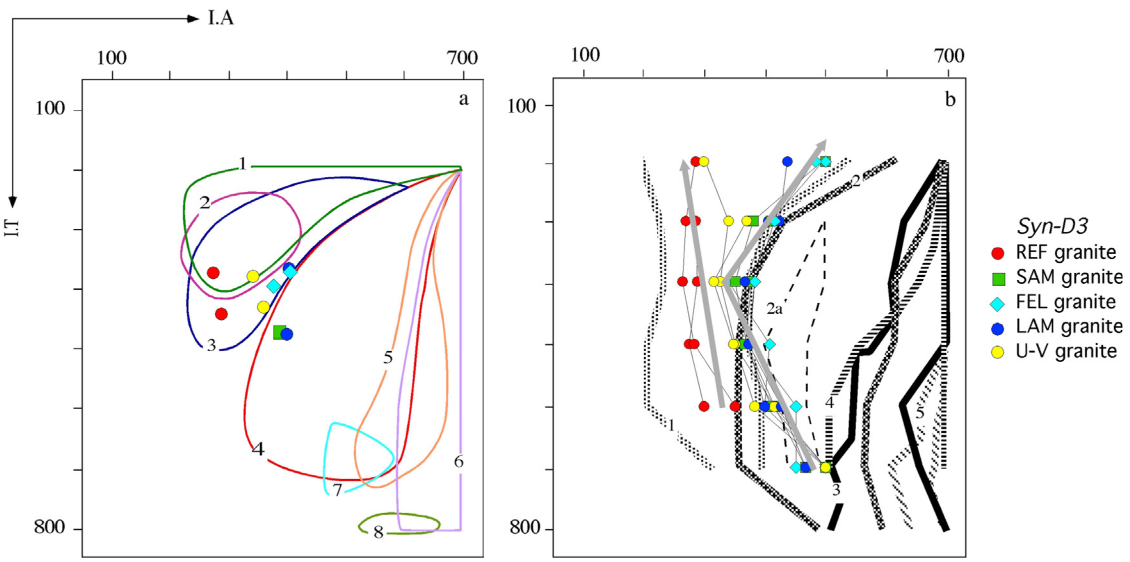

Fig. 3. (Color online.) Morphological signatures of zircon populations from syn-D_3 granites in the (A, T) morphological diagram (Pupin, 1988). a. Distribution of the mean point; granitic domains: (1) aluminous leucogranites; (2) (sub) autochthonous anatectic granites; (3) intrusive aluminous monzogranites–granodiorites; (4) calc-alkaline and K-calc-alkaline series; (5) sub-alkaline series; (6) alkaline series; (7) continental tholeiitic series; (8) oceanic plagiogranites. b. (TET) Typological evolutionary trends; Granitic domains: (1) crustal or mainly crustal origin; (2) calc-alkaline granites;(2a) K-calc-alkaline granites; (3) sub-alkaline granites; (4) alkaline subsolvus granites; (5) alkaline hypersolvus granites. The arrows indicate the typological evolution's direction.

5.1.2. Late-D3 biotite-dominant granitoids

According to their typological distribution, the zircons of the late-tectonic granites are dominantly of subtypes S2, S3, S7, S12, and S17 (Fig. 2) for the Vieira do Minho granite, having an almost equally well-developed {100} and {110} prisms, with a slightly predominance of the latter, which give a mean IT index in the range of 384 to 405 (Fig. 4a). Most of zircons present the {211} pyramid more developed than the {101} one, and accordingly a low IA index, 321–331 (Fig. 4a). In the Moreira de Rei granite, we can distinguish two different typological distributions: one is dominantly of subtypes S12, S13, and S17, typical of calc-alkaline granites (Pupin, 1988), and the other belong to the S3 and L3 types (Fig. 2). These typological distributions imply a similar dominance of the two prisms and the two pyramids, as found in the Vieira do Minho granite, but with some minor development of the {110} prism and the {101} pyramid. Therefore the MR granite has mean index values of IT = 452 and of IA = 349, slightly higher than those recorded for the VM granite (Fig. 4a). The zircon population from the Vieira do Minho granite reveals characteristics of aluminous monzogranites, but overlapping several typological domains (Fig. 4). On the other hand, the morphological characteristic of zircons from the Moreira de Rei granite seems to indicate also typological characteristics typical of aluminous monzogranites–granodiorites (Fig. 4), but closer to those of zircons from calc-alkaline granites (Pupin, 1988).

5.1.3. Post-D3 biotite granitoids

The crystal morphology of these granites is very distinctive compared to that of the other granites studied. The zircon population from the Vila Pouca de Aguiar granite and Pedras Salgadas granite shows a great variety of subtypes, which are more concentrated in the right-hand side of the zircon typological diagram (Pupin, 1980), especially the Pedras Salgadas granite zircons. In the Vila Pouca de Aguiar granite, the zircon morphology goes from subtypes S17, S18, S24 to S19, S22, S23, S25 (Fig. 2), and thus the {100} prism and {101} pyramid are more dominant than {110} prism and {211} pyramid, which according to Pupin's scale, are characteristic of calc-alkaline granodiorites of hybrid (crustal and mantle) origin (Fig. 4). Other zircons belong to G1, P1 and P2 morphological types (Fig. 2), with only a well-developed {101} pyramid and a less pronounced {100} prism, formed in sub-alkaline and alkaline series of crustal-plus-mantle or mainly mantle origin, in accordance with the genetic classification (Fig. 4). The Pedras Salgadas granite zircons are dominantly G1, P1, show a well-developed {100} prism and a single {101} pyramid typical of zircon from "granitoids of mainly mantle origin", followed by subtypes S19, S24, and S25 (Fig. 2), typical of zircons found in calc-alkaline granodiorites or sub-alkaline granitoids. This crystal morphology corresponds to a well-developed {100} prism and {101} pyramid with supplementary {211} pyramid and {110} prism.

The zircon typological distribution in the Vila Pouca de Aguiar granite is expressed in mean IA and IT index values of 487 and 550, respectively, whereas in the Pedras Salgadas granite the IA index has a value close to 600, pointing to a more alkaline nature, and an IT index slightly low (IT = 472). The mean point indicates that the Pedras Salgadas granite belongs to the group of sub-alkaline granites (Fig. 4a).

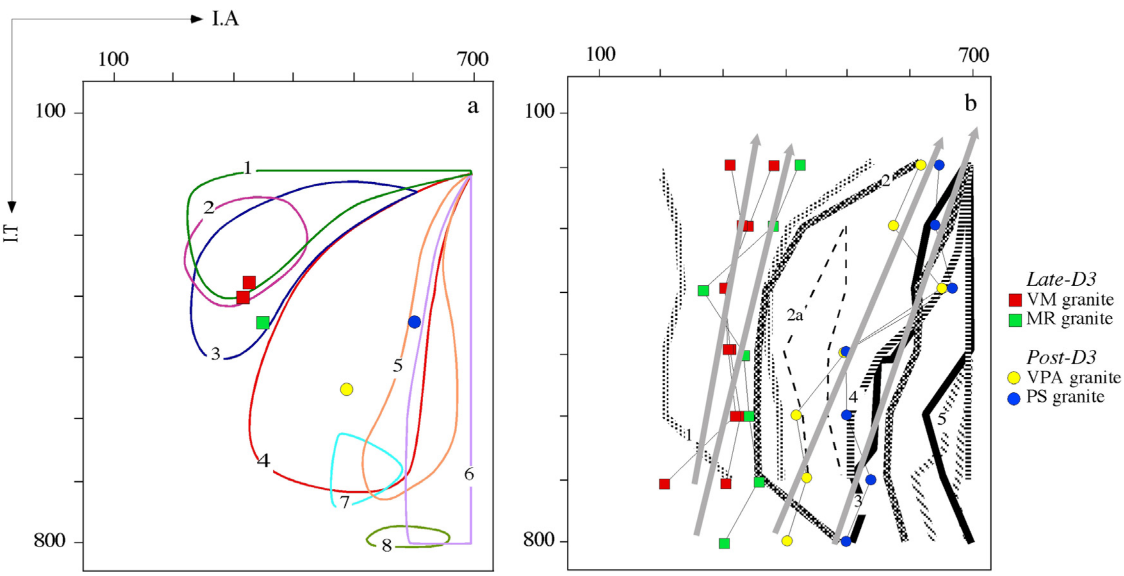

Fig. 4. (Color online.) Morphological signatures of zircon populations from late- and post-D_3 granites in the (A, T) morphological diagram (Pupin, 1988). a. Distribution of the mean point; granitic domains: (1) aluminous leucogranites; (2) (sub)autochthonous anatectic granites; (3) intrusive aluminous monzogranites-granodiorites; (4) calc-alkaline and K-calc-alkaline series; (5) sub-alkaline series; (6) alkaline series; (7) continental tholeiitic series; (8) oceanic plagiogranites. b. Typological evolutionary trends (TET); granitic domains: (1) crustal or mainly crustal origin; (2) calc-alkaline granites; (2a) K-calc-alkaline granites; (3) sub-alkaline granites; (4) alkaline subsolvus granites; (5) alkaline hypersolvus granites. The arrows indicate the typological evolution direction.

6. Internal structures

6.1. Syn-D_3 biotite granitoids

The study carried out by BSE reveals that the zircons have internal structures that are typically magmatic, with magmatic zoning and nebulitic structures.

The nebulitic structures are characterised by diffuse structures (Fig. 5a), which are more prevalent in less evolved types (subtypes S24, S18).

Magmatic zoning is thin, sometimes wavy, and occur in zircons of all granites (Fig. 5b–d). In the Refoios do Lima granite, zircons are characterised by a thin magmatic zoning, with rare nebulitic structures.

Zircons with elongated and short prisms reveal identical structures (magmatic zoning and/or nebulitic structures) (Fig. 5b), while the subspherical multifaceted zircons have poorly defined nuclei, surrounded by a magmatic zoning, sometimes weak.

The zircons with lamellar form, common in Ucanha–Vilar and Lamego granites, reveal a thin magmatic zoning with frequent inclusions of biotite.

Sometimes we can see internal morphological evolutions shown by different kinds of magmatic zoning. In zircon 5b (Sameiro granite), in the inner zone, the pyramidal face is {101}, evolved to {211} in the direction of the outer zone (S9 → S2), indicating a reaction with the melt.

Some zircons also record complex histories involving fracturing and consolidation of broken crystals, like in zircon 5c (Felgueiras granite).

In Sameiro, Felgueiras, Lamego and Ucanha–Vilar granites, zircons are characterised mainly by two stages of formation (Fig. 5b and c):

- an inner zone, with nebulitic or without internal structure in less developed morphological types or a zoning in the more evolved morphological types, with rounded shapes in the area of the pyramidal faces, sometimes with the zoning truncated;
- an outer zone, with magmatic zoning.

This type of structure indicates a reaction step with the magmatic environment.

Relic cores were also identified like in Sameiro granite, where some zircons show relic cores, indicating the presence of inherited zircons (Fig. 5d). The presence of these inherited zircons in Sameiro granite is responsible for the existence of a reverse discordia according to a geochronological study on U–Pb analysis of multi-grain zircon and monazite fractions (Dias et al., 1998). Relic nuclei were also identified in zircons from Refoios Lima, Sameiro, Felgueiras and Lamego granites through the observation of their internal structure by cathodoluminescence. Zircons with inherited cores were not detected in the Ucanha–Vilar granite. The occurrence of these relict nuclei are more frequently in the zircons of the Refoios do Lima granite and less in the Lamego granite, showing a geographic decrease from north to south.

6.2. Late-D3 biotite-dominant granitoids

According to their morphology, four different populations of zircon have been recognized in these granitoids: prismatic zircons (short, long and acicular), lamellar zircons and a less common subspherical multifaceted zircon. The internal structures (BSE images) of the zircons from both granites are very similar and present typical magmatic patterns. Generally they consist of an unzoned to weakly zoned core surrounded by a rim of euhedral regular fine oscillatory zoned zircon (Fig. 5e and g). Zircon **e** is a crystal from the VM granite that shows a well-developed {110} prism and two pyramids {101} and {211}, with the {211} pyramid more dominant, corresponding to subtype S2/S3. Zircon **g** (MR granite) has an inner well-developed {110} prism and {211} pyramid. The {100} prism and the {101} pyramid are subordinate (subtype S3/S4) and are overgrown by a single {110} prism and an almost equal development of the {211} and {101} pyramids, subtype L2/L3.

In some zircons, that rim is in turn surrounded by a weakly zoned outer rim (Fig. 5f), which is interpreted to have formed by recrystallization of the primary zircon grown during the cooling of the granite (Pidgeon et al., 1998). Zircon **f** (VM granite) has an inner zone with equal development of the two prisms {110} and {100}, and the {211} pyramid slightly predominant over {101} belongs to subtype S12. This morphological type is surrounded by a S7/S2 subtype with a {100} prism more subordinate. The BSE images also show a clear growth discontinuity between a partially resorbed inner zone with faint zoning, and a finely zoned outer zone (Fig. 5h). These structures are interpreted as magmatic, probably developed in two crystallization steps and revealing some disequilibrium between the early generation and the liquid. These structures are common in prismatic zircons. Zircon **h** (MR granite) is a subtype S7/S2, in which there is a certain equilibrium in the development of the two pyramids, with predominance of the {110} prism. The acicular and the lamellar zircons are very homogeneous crystals devoid of cores and showing generally a faint zoning with dominantly oscillatory internal structures. The BSE imaging of the subspherical type reveals the presence of inherited cores, surrounded by finely zoned rims.

6.3. Post-D3 biotite granitoids

Morphological study has allowed the identification of different types of zircon, prismatic zircons (short, long and acicular) and lamellar zircons.

Zircons from this group of granites show a much more regular zoning than the other groups. In the Vila Pouca de Aguiar, the BSE images of the prismatic zircons revealed an inner zone surrounded by a well-developed magmatic oscillatory zoning as a result of heterogeneous trace element distribution (Martins et al., submitted) (Fig. 5i and j). Zircon **i** (VPA granite) is a crystal showing an inner zone with a well-developed {100} prism and equally well-developed {211} and {101} pyramids (subtype S23) overgrown by a S15 subtype, whereas zircon crystal **j**

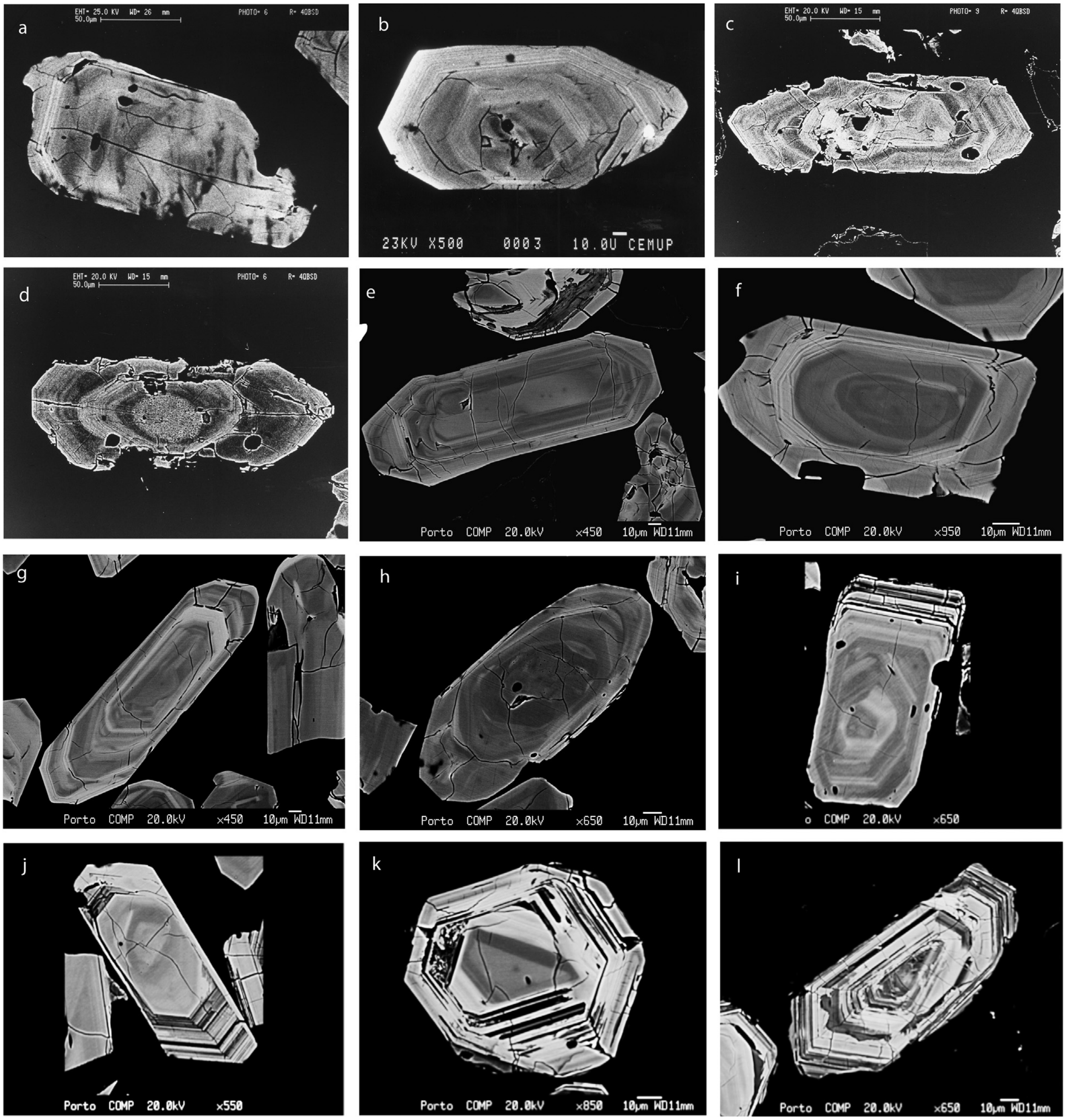

Fig. 5. Back-scattered electron microscopy images showing the range of textures observed in zircons from syn- (**a** to **d**) late- (**e** to **h**) and post-D3 (**i** to **l**) granites. (**a**) An inner zone with nebulitic structure followed by a fine magmatic zoning (S5, Lamego granite); (**b**) internal morphological evolution shown by different magmatic zoning: in the inner zone, the pyramidal face is (101), evolving to (211) in the direction of the outer zone (S9 → S2, Sameiro granite); (**c**) fine magmatic zoning in the inner zone with truncation by a darker zone, with rounded shapes in the area of the pyramidal faces, followed by new zoning in the outermost zone (S2, Felgueiras granite); (**d**) some zircons show relic cores indicating the presence of inherited zircons, followed by a magmatic zoning (S2, Sameiro granite); (**e**) weakly zoned core surrounded by a fine oscillatory rim (S2/S3 VM granite); (**f**) unzoned core followed by fine oscillatory zone, which in turn is surrounded by a weakly zoned outer rim (S12 → S7/S2, VM granite); (**g**) grain with euhedral regular fine magmatic zoning, but with different morphologies from the inner to the outer zone (S3/S4 → L2/L3, MR granite); (**h**) growth discontinuity between a partially resorbed core with faint zoning and a finely zoned outer zone (S7/S2, MR granite); (**i**) internal morphological evolution showing different magmatic zoning processes, S23 inner zone surrounded by S15 outer zone (VPA granite); (**j**) a weakly zoned core surrounded by an outer rim of oscillatory zone (P1, VPA granite); (**k**) an inner zone with faint zoning surrounded by well-developed oscillatory zoning (S24→S15, PS granite); (**l**) well-developed oscillatory zoning (P1, PS granite).

(VPA granite) is a P1 subtype, and thus shows a well-developed {110} prism and a single {101} pyramid.

Some zircons have cores, which could correspond to an earlier magmatic crystallization (Pidgeon, 1992), sometimes partially resorbed and with a faint zoning. In the Pedras Salgadas granite zircons are characterised by an external well-developed magmatic oscillatory zoning, which is interpreted as typical of primary, magmatic zoning (Fig. 5k and l). Zircon **k** presents an inner zone with a well-developed {110} prism (subtype S24) evolving to the outer zone to an equal development of the two prims and a {101} pyramidal face more dominant (S15 subtype); zircon **l** has a well-developed {110} prism and a single {101} pyramid (subtype P1).

The acicular and lamellar zircons are in general unzoned to weakly zoned, and lack magmatic overgrowths.

7. Discussion and conclusions

The zircon crystallization history may give insights into magma petrogenesis, provided that the magma system is reasonably well characterised geochemically and isotopically (Gagnevin et al., 2010). In such cases, the zircon's external morphology combined with internal structures has the ability to record magma evolution histories, from its initial formation by source melting, contamination and mixing with different magma batches, fractional crystallization and differentiation and final emplacement or extrusion (Corfu et al., 2003). Typological characteristics of zircon crystals may display modifications closely related to compositional evolutions of granitoids, and these changes through magmatic evolution can be seen in single crystals of zircon (Belousova et al., 2006; Siebel et al., 2006) and in the morphological evolution of the population. There is a general agreement that melt composition controls zircon morphology, although different views exist as to which elements govern the development of zircon crystal faces (e.g., Benisek and Finger, 1993; Pupin, 1980; Vavra, 1990, 1994). Zircon typological studies as proposed by Pupin (1980) can help us to understand the evolution of granitoids, especially when they are combined with detailed internal structures (e.g., Köksal et al., 2008). The typological trends in studied granites suggest that the composition of zircon evolves as the magma cools and becomes more aluminous or more alkaline, namely with a trend towards a decrease in the crystallization temperature (Fig. 3b and Fig. 4b). However, for specific cases, e.g., when new batches of hotter magma occur, an opposite trend is observed (Belousova et al., 2006). Zircons with different initial and final compositions, or morphologies, imply a mixing between two distinct sources, which is also corroborated by their typological evolutionary trends. According Belousova et al. (2006), changes in zircon morphology within single grains and between populations reflect the mixing of magmas and changes in the composition of the magma through mingling processes and progressive crystallization.

7.1. Syn-D3 biotite granitoids

Zircon grains from the Refoios de Lima granite show gradual changes in their morphology, whereas in Sameiro, Felgueiras, Lamego and Ucanha–Vilar granites they have a more complex morphology (internal and external), which reflects modifications in the composition of the magma and provides a qualitative record of magma evolution. The typological population and typological evolutionary trend (TET) of zircons from Refoios do Lima (REF) granite takes place over an area indicating that this granite has a mainly crustal origin (Fig. 3b), with equally well-developed {100} and {110} prism, with a predominance of the latter, indicating an aluminous environment of formation. This typological distribution is similar to what happens to monzogranites and granodiorites of Margeride type (Pupin, 1976, 1980) whose typological characteristics of zircon are identical to those of zircons from the Refoios do Lima granite. Crystalline groupings parallel to the crystallographic axis *c* are also frequent in the Refoios de Lima granite (Simões, 2000), reinforcing the hypothesis of a crustal origin. This is in agreement with mineralogical, geochemical and isotopic studies for Refois do Lima granite (Dias et al., 2002; Simões, 2000) that confirmed an origin from crustal-derived melts. In fact, the isotopic composition of Refoios do Lima granite (Sr_i = 0.7104–0.7106; ε_{Nd} = –6.0 to –6.3) shows a signature that is typical of crustal materials.

For zircons of Sameiro (SAM), Felgueiras (FEL), Lamego (LAM) and Ucanha–Vilar (U–V) granites, the typological evolutionary trends cross the domain of the calc-alkaline granites to the aluminous granites, contrary to what would be expected from a simple evolutionary crystallization process (Fig. 3b). This may be interpreted as indicating a mixing process between two compositionally distinct magmas, which could explain those typological evolutions. In fact, the presence of gabbros in the region where the Sameiro granite outcrops originated from an enriched mantle (Dias and Leterrier, 1994), and from the presence of granodiorites–quartz monzodiorites in the Ucanha–Vilar area, as well as the occurrence of mafic microgranular enclaves in the Sameiro, Felgueiras, Lamego, and Ucanha–Vilar granites, supports a mixing model for their genesis, involving a basic magma (probably a mantle-derived magma) and a felsic crustal magma. This is also supported by geochemical and isotopic studies of these granites (Dias et al., 2002; Simões, 2000). So, the typological evolutionary trends (TET) and the fact that some zircons are characterised by two stages of formation can be interpreted as a mixing process, which is in good accordance with mineralogical, chemical and isotopic composition of those granites (Dias et al., 2002; Simões et al., 1997; Simões, 2000).

7.2. Late-D3 biotite granitoids

The gradual change in morphology of the late-D_3 biotite-dominant granitoids suggests that zircon was crystallizing as the magma cooled and there is no evidence supporting abrupt changes in magma composition. Moreover, the internal structures shown in Fig. 5 as well as the evolutionary trends (Fig. 4b) within the zircon crystals mimic the TETs displayed by the zircon population to which they belong. Effectively, zircon **f** (Vieira do Minho granite) and zircon **g** (Moreira de Rei granite) are very good examples. Zircon **f** has an inner zone belonging to the subtype S12, which is surrounded by a S7/S2 subtype. Zircon **g** has an inner well-developed {110} prism and {211} pyramid (subtype S3/S4), and is overgrown by a single {110} prism and an almost equal development of the {211} and {101} pyramids, subtype L2/L3. The morphological signatures of these zircon grains, namely the mean point and typological evolutionary trends (Fig. 4), with almost constant IAs during their evolution, indicate a crustal or dominantly crustal origin for the VM and the MR granites. The evolution in zircon morphology suggests the crystallization and/or the fractionation of two magmas during a general decrease in temperature. There is no evidence of magma mixing in these samples and the whole process is consistent with control by fractional crystallization during cooling. This is also supported by geochemical and isotopic data, as discussed by Martins et al. (2013), who argued that the granites from the Vieira do Minho pluton were probably derived from crustal protoliths, although at different crustal levels.

7.3. Post-D3 biotite granitoids

Finally, the post-D_3 biotite granitoids show narrowly-spaced uninterrupted oscillatory patterns representing higher degrees of zircon saturation (supersaturation) (Hoskin and Schaltegger, 2003). According to Clairborne et al. (2010 and references therein), oscillatory zoning represents kinetic effects at the crystal-melt interface, dependent on the ordering in the melt by polymerization and often promoting local supersaturation and disequilibrium, rather than rapid changes in the composition or conditions in the bulk melt. The zircon typology of these granites is quite different from the previous ones, exhibiting significantly different mean points and TETs (Fig. 4). The typological evolutionary trends are characterised by increasing IAs for decreasing ITs. The morphological types are found in calc-alkaline and in sub-alkaline granites and both define typological evolutionary trends that begin in the calc-alkaline domain and extend towards the sub-alkaline one (Fig. 4b). The Pedras Salgadas IA index has a higher value than Vila Pouca de Aguiar, pointing to a more alkaline nature and accordingly the mean point indicates that the Pedras Salgadas granite belongs to the sub-alkaline granites. Thus, the zircon morphological characteristics of the VPA and the PS granites follow the calc-alkaline/sub-alkaline trend, and the source rock, according to Pupin' scheme, could be a hybrid of mantle and crustal origin or mainly of mantle origin, typical of I-type granitoids (Fig. 4).

The internal structures show convincingly which type is changing continuously as the magma cooled and became more alkaline, as documented by one Vila Pouca de Aguiar crystal (Fig. 5i) and by others from the Pedras Salgadas granite (Fig. 5k). These crystals show a significant change in morphology from inner to outer zones (zircon i S23→S15; zircon k S24→S15), representing a change in the crystal morphology during crystal growth. Nevertheless, other crystals (Fig. 5j and l) have kept the same typology throughout the crystallization process.

The petrogenetic model proposed for the zircons typologically studied in these granites is in accordance with geochemical and isotopic data. The trends for major and trace elements in the Vila Pouca de Aguiar and the Pedras Salgadas granites are consistent with the fact they belong to the I-type. This is also supported by their weakly evolved isotopic compositions; the VPA granite presents a $(^{87}Sr/^{86}Sr)_{299}$ between 0.7067 and 0.7071, whereas $\varepsilon_{Nd_{299}}$ is around −2.5 (Martins et al., 2009). The PS granite yields the less evolved isotopic composition with $(^{87}Sr/^{86}Sr)_{299}$ ranging from 0.7044 and 0.7050 and $\varepsilon_{Nd_{299}}$ = −2.0. Therefore, an origin by mantle input with local intermingling with crustal sources has been proposed (Martins et al., 2009).

The geochemical and isotopic data measured in these granites are consistent with the typological study of their zircon populations. This fact shows that the morphology of zircons populations can be used with a high degree of certainty to determine the origin and evolution of granitic magmas in a quick and inexpensive way. Moreover, the evidence that internal evolution within a single crystal mimics the typological evolutionary trends in all granites studied corresponds to an important step in the knowledge of zircon growth within silicic melts.

The knowledge of the crystal morphology of zircons and of their internal structures is crucial for the interpretation of U–Pb zircon geochronology and Hf isotope studies, because zircons commonly show heterogeneous growth zones, and thus it is important to have the ages and Hf isotopes analyzed within the same zones. Therefore, their crystal morphology and their internal structures could be an important clue to understand which processes lead to the wide scatter of ages and Hf isotopes, as it has been highlighted in several papers (e.g., Belousova et al., 2009; Condie et al., 2005; Gerdes and Zeh, 2009; Hawkesworth and Kemp, 2006; Kurhila et al., 2010; Orejana et al., 2011; Shaw et al., 2011; Villaseca et al., 2012).

Acknowledgements

This work is integrated in the activities of the "Centro de Geologia da Universidade do Porto", with the financial support of the PEst-OE/CTE/UI0039/2011-2014 (Portuguese Foundation of Technology). The authors thank to CEMUP and LNEG for the BSE analyses. We are also grateful to Fernando Corfu for his comments on internal structures. Helpful and constructive reviews by Bernard Bonin, Elena Belousova and the editor Marguerite Godard are gratefully acknowledged.

References

Almeida, A., Martins, H.C.B., Noronha, F., 2002. Hercynian acid magmatism and related mineralisations in northern Portugal. Gondwana Res. 5 (2), 423–434.
Bard, J.P., Matte, P., Ribeiro, A., 1980. La chaîne hercynienne d'Europe occidentale en termes de tectonique des plaques. Mem. BRGM 108, 233–246.
Belousova, E.A., Griffin, W.L., O'Reilly, S.Y., 2006. Zircon crystal morphology, trace element signatures and Hf isotope composition as a tool for petrogenetic modelling: examples from eastern Australian granitoids. J. Petrol. 47 (2), 329–353.
Belousova, E.A., Reid, A.J., Griffin, W.L., O'Reilly, S.Y., 2009. Rejuvenation vs. recycling of Archean crust in the Gawler Craton, South Australia: Evidence from U–Pb and Hf isotopes in detrital zircon. Lithos 113 (3–4), 570–582.

Benisek, A., Finger, F., 1993. Factors controlling the development of prism faces in granite zircons- a microprobe study. Contrib. Mineral. Petrol. 114 (2), 441–451.

Clairborne, L.L., Miller, C.F., Wooden, J.L., 2010. Trace element composition of igneous zircon: a thermal and compositional record of the accumulation and evolution of a large silicic batholith, Spirit Mountain. Nevada. Contrib. Mineral. Petrol. 160, 511–531.

Condie, K.C., Beyer, E., Belousova, E.A., Griffin, W.L., 2005. U–Pb isotopic ages and Hf isotopic composition of single zircons: the search for juvenile Precambrian continental crust. Precambrian Res. 139, 42–100.

Corfu, F., Hanchar, J.M., Hoskin, P.W.O., Kinny, P., 2003. Atlas of zircon textures. In: Hanchar, J.M., Hoskin, P.W.O. (Eds.), Zircon. Rev. Miner. Geochem., 53, pp. 469–500.

Dias, G., Leterrier, J., 1994. The genesis of felsic-mafic plutonic associations: a Sr and Nd isotopic study of the Hercynian Braga granitoid massif (northern Portugal). Lithos 32, 207–223.

Dias, G., Ribeiro, A., 1995. The Ibero-Armorican Arc: a collision effect against an irregular continent? Tectonophysics 246, 113–128.

Dias, G., Leterrier, J., Mendes, A., Simões, P., Bertrand, J.-M., 1998. U–Pb zircon and monazite geochronology of syn- to post-tectonic Hercynian granitoids from the Central Iberian Zone (Northern Portugal). Lithos 45, 349–369.

Dias, G., Simões, P.P., Ferreira, N., Leterrier, J., 2002. Mantle and crustal sources in the genesis of Late-Hercynian granitoids (NW Portugal): geochemical and Sr–Nd isotopic constraints. Gondwana Res. 5 (2), 287–305.

Ferreira, N., Iglésias, M., Noronha, F., Pereira, E., Ribeiro, A., Ribeiro, M.L., 1987. Granitos da Zona Centro Ibérica e seu enquadramento geodinâmico. In: Bea, F., Carnicero, A., Gonzalo, Lopez Plaza, J.M., Rodriguez Alonso, M. (Eds.), Geología de los Granitoides y Rocas Asociadas del Macizo Hesperico. Editorial Rueda, Madrid, (Libro de Homenaje a L.C. García de Figuerola), pp. 37–51.

Frost, B.R., Barnes, C.G., Collins, W.J., Arculus, R.J., Ellis, D.J., Frost, C.D., 2001. A geochemical classification for granitic rocks. J. Petrol. 42 (11), 2033–2048.

Gagnevin, D., Daly, J.S., Kronz, A., 2010. Zircon texture and chemical composition as a guide to magmatic processes and mixing in a granitic environment and coeval volcanic system. Contrib. Mineral. Petrol. 159, 579–596.

Gerdes, A., Zeh, A., 2009. Zircon formation versus zircon alteration – New insights from combined U–Pb and Lu–Hf in-situ LA-ICP-MS analyses, and consequences for the interpretation of Archean zircon from the Central Zone of the Limpopo Belt. Chem. Geol. 261 (3–4), 230–243.

Hawkesworth, C.J., Kemp, A.I.S., 2006. Using hafnium and oxygen isotopes in zircons to unravel the record of crustal evolution. Chem. Geol. 226, 144–162.

Hoskin, P.W.O., Schaltegger, U., 2003. The composition of zircon and igneous and metamorphic petrogenesis. In: Hanchar, J.M., Hoskin, P.W.O. (Eds.), Zircon. Rev. Miner. Geochem., 53, pp. 27–62.

Köksal, S., Cemal Göncüoglu, M., Toksoy- Köksal, F., Möller, A., Kemnitz, H., 2008. Zircon typologies and internal structures as petrogenetic indicators in contrasting granitoid types from central Anatolia. Turkey. Mineral. Petrol. 93, 185–211.

Kurhila, M., Andersen, T., Tapani Rämö, O., 2010. Diverse sources of crustal granitic magma: Lu–Hf isotope data on zircon in three Paleoproterozoic leucogranites of southern Finland. Lithos 115, 263–271.

Lagarde, J.-L., Capdevila, R., Fourcade, S., 1992. Granites et collision continentale : l'exemple des granitoides carboniferes dans la chaîne hercynienne ouest-européenne. Bull. Soc. geol. France 163 (5), 597–610.

Martins, H.C.B., Sant'Ovaia, H., Noronha, F., 2007. Post-tectonic granite intrusion controlled by a deep Variscan fault in northern Portugal, 32, Cadernos Lab. Xeolóxico de Laxe, España, pp. 221–235.

Martins, H.C.B., Sant'Ovaia, H., Noronha, F., 2009. Genesis and emplacement of felsic Variscan plutons within a deep crustal lineation, the Penacova-Régua-Verín fault: an integrated geophysics and geochemical study (NW Iberian Peninsula). Lithos 111, 142–155.

Martins, H.C.B., Sant'Ovaia, H., Abreu, J., Oliveira, M., Noronha, F., 2011. Emplacement of the Lavadores granite (NW Portugal): U/Pb and AMS results. C. R. Geoscience 343, 387–396.

Martins, H.C.B., Sant'Ovaia, H., Noronha, F., 2013. Late-Variscan emplacement and genesis of the Vieira do Minho composite pluton, Central Iberian Zone: Constraints from U–Pb zircon geochronology, AMS data and Sr–Nd–O isotope geochemistry. Lithos 162/163, 221–235.

Matte, P., 1991. Accretionary history and crustal evolution of the Variscan Belt in western Europe. Tectonophysics 196, 309–337.

Noronha, F., Ramos, J.M.F., Rebelo, J.A., Ribeiro, A., Ribeiro, M.L., 1979. Essai de corrélation des phases de déformation hercynienne dans le Nord-Ouest péninsulaire. Bol. Soc. Geol. Portugal 21, 227–237.

Orejana, D., Villaseca, C., Armstrong, R.A., Jeffries, T.E., 2011. Geochronology and trace element chemistry of zircon and garnet from granulite xenoliths: Constraints on the tectonothermal evolution of the lower crust under central Spain. Lithos 124, 103–116.

Pidgeon, R.T., 1992. Recrystallization of oscillatory zoned zircon: some geochronological and petrological implications. Contrib. Mineral. Petrol. 110, 463–472.

Pidgeon, R.T., Nemchin, A.A., Hitchen, G.J., 1998. Internal structures of zircons from Archaen granites from the Darling Range batholith: implications for zircon stability and interpretation of zircon U-Pb ages. Contrib. Mineral. Petrol. 132, 288–299.

Pupin, J.-P., 1976. Signification des caractères morphologiques du zircon commun des roches en pétrologie. Base de la méthode typologique. Applications (Thèse d'État). Université de Nice (394 p.).

Pupin, J.-P., 1980. Zircon and granite petrology. Contrib. Mineral. Petrol. 110, 463–472.

Pupin, J.-P., 1985. Magmatic zoning of Hercynian Granitoïds in France based on zircon typology. Schweiz. Mineral. Petrogr. Mitt. 65, 29–56.

Pupin, J.-P., 1988. Granites as indicators in paleogeodynamics. Rend. Soc. Ital. Mineral. Petrol. 43 (2), 237–262.

Pupin, J.-P., Turco, G., 1972. Une typologie originale du zircon accessoire. Bull. Soc. Fr. Mineral. Cristallogr. 95, 348–359.

Pupin, J.-P., Turco, G., 1975. Typologie du zircon accessoire dans les roches plutoniques, dioritiques, granitiques et syénitiques. Facteurs essentiels déterminant les variations typologiques. Petrologie I (2), 139–156.

Ribeiro, A., Iglesias, M., Ribeiro, M.L., Pereira, E., 1983. Modèle géodynamique des Hercynides Ibériques. Comm. Serv. Geol. Portugal 6, 191–214.

Ribeiro, A., Quesada, C., Dallmeyer, R.D., 1990. Geodynamic evolution of the Iberian Massif. In: Dallmeyer, R.D., Martinez Garcia, (Eds.), Pre-Mesozoic Geology of Iberia. Springer-Verlag, Berlin, pp. 399–409.

Shaw, S.E., Flood, R.H., Pearson, N.J., 2011. The new England Batholith of eastern Australia: evidence of silicic magma mixing from zircon $^{176}Hf/^{177}Hf$ ratios. Lithos 126, 115–126.

Siebel, W., Thiel, M., Chen, F., 2006. Zircon geochronology and compositional record of late- to post-kinematic granitoids associated with the Bavarian Pfahl zone (Bavarian Forest). Mineral. Petrol. 86, 45–62.

Simões, P.P., 2000. Instalação, geocronologia e petrogénese de granitóides biotíticos sintectónicos associados ao cisalhamento Vigo-Régua (ZCI, Norte de Portugal) (Ph.D. Thesis [Unpubl.]). Univ. do Minho, Braga, Portugal (351 p.).

Simões, P.P., Pupin, J.-P., Dias, G., 1997. Utilização do zircão como indicador genético e evolutivo em granitóides hercínicos biotíticos associados ao cisalhamento Vigo-Régua (Norte de Portugal). In: Actas X Semana de Geoquímica/IV Congresso de Geoquímica dos Países de Língua Portuguesa, Braga, Portugal, pp. 147–150.

Vavra, G., 1990. On the kinematics of zircon growth and its petrogenetic significance: a cathodoluminescence study. Contrib. Mineral. Petrol. 106, 90–99.

Vavra, G., 1993. A guide to quantitative morphology of accessory zircon. Chem. Geol. 110, 15–28.

Vavra, G., 1994. Systematics of internal zircon morphology in major Variscan granitoid types. Contrib. Mineral. Petrol. 117, 331–344.

Villaseca, C., Orejana, D., Belousova, E.A., 2012. Recycled metaigneous crustal sources for S- and I-type Variscan granitoids from the Spanish Central System batholith: Constraints from Hf isotope zircon composition. Lithos 153, 84–93.